

1 **Post-print**

- 2 Malusà, M. G., Anfinson, O. A., Dáfov, L. N., & Stockli, D. F. (2016).
3 Tracking Adria indentation beneath the Alps by detrital
4 zircon U-Pb geochronology: Implications for the
5 Oligocene–Miocene dynamics of the Adriatic microplate.
6 Geology, 44(2), 155-158.
7 *DOI:10.1130/G37407.1*

8 Tracking Adria indentation beneath the Alps by detrital
9 zircon U-Pb geochronology: Implications for the Oligo-
10 Miocene dynamics of the Adriatic microplate

11 **Marco G. Malusà¹, Owen A. Anfinson^{2,3}, Laura N. Dáfov², and Daniel F. Stockli²**

12 *¹Department of Earth and Environmental Sciences, University of Milano-Bicocca, Piazza
13 della Scienza 4, 20126 Milan, Italy*

14 *²Department of Geological Sciences, University of Texas at Austin, 1 University Station
15 C1100, Austin, Texas 78712, USA*

16 *³Department of Geology, Sonoma State University, 1801 East Cotati Avenue, Rohnert
17 Park, California 94928, USA*

18 **ABSTRACT**

19 The Adriatic microplate is a key player in the Western Mediterranean tectonic
20 puzzle, but its Oligo-Miocene dynamics is not yet fully understood. In fact, even though
21 the timing and magnitude of Adriatic slab rollback and backarc extension in the
22 Apennines have long been established, the timing of progressive Adria indentation
23 beneath the Central Alps and of major strike-slip motion along the Insubric Fault are still
24 poorly constrained. Here, we tackle these issues by utilizing detrital zircon U-Pb
25 geochronology on Adriatic foredeep turbidites, i.e., by comparing the geochronologic
26 fingerprints of the exhuming tectonic domes of the Central Alps (Ticino and Toce
27 subdomes) with those of the Oligo-Miocene turbidites chiefly derived from their erosion.
28 We analyzed 11 sandstone samples ranging in age from 32 to 18 Ma. The ratio between
29 Variscan and Caledonian zircon grains (which are dominant in the Toce and Ticino

30 subdomes, respectively) sharply increases at ~24–23 Ma. This major provenance change
31 marks the westward shift of the Adriatic indenter beneath the Central Alps, and the
32 associated right-lateral activity of the Insubric Fault. Coexistence of strike-slip motion at
33 the northern boundary of the Adriatic microplate at ~24–23 Ma, and of trench retreat
34 during scissor-type backarc opening to the west, requires a near-vertical rotation axis
35 located at the northern tip of the Ligurian-Provençal basin. We propose that the rotation
36 axis position was controlled by the interaction between the European and the Adriatic
37 slabs, which may have collided at depth by the end of the Oligocene triggering the
38 westward shift of the Adriatic indenter beneath the Central Alps.

39 INTRODUCTION

40 The Adriatic microplate is a key piece in the complex Western Mediterranean
41 tectonic puzzle (Fig. 1). It represents the lower plate of the Apenninic belt to the SW, the
42 lower plate of the Dinaric belt to the NE, and the upper plate of the Alpine belt to the
43 NW, where it is indented north of the Insubric Fault beneath the metamorphic units of the
44 Lepontine Dome (X-X' in Fig. 1) (Handy et al., 2010; Malusà et al., 2015). The motion
45 of the Adriatic microplate relative to Europe during the Cenozoic is reasonably well
46 constrained (e.g., Dewey et al., 1989), as is the timing and magnitude of Neogene slab
47 rollback and trench retreat in the Apennines (Faccenna et al., 2001; Gattacceca et al.,
48 2007). By contrast, no reliable time constraint is available in the Central Alps for the
49 progressive westward migration of the Adriatic indenter beneath the Lepontine Dome
50 (Merle et al., 1989; Steck and Hunziker, 1994), and for the associated Oligo-Miocene
51 strike-slip motion along the Insubric Fault (Schmid et al., 1989; Zwingmann and
52 Mancktelow, 2004). Such a paucity of kinematic constraints along the northern boundary

53 of the Adriatic microplate prevents reliable analysis of slab dynamics during trench
54 retreat and backarc extension.

55 Here, we use detrital zircon U-Pb geochronology on foredeep turbidites to track
56 Adria indentation beneath the Central Alps, and provide first time constraints for major
57 strike-slip motion along the Insubric Fault. Results are integrated with available
58 kinematic constraints for the Western Mediterranean area, shedding light on the Oligo-
59 Miocene dynamics of the Adriatic microplate and on its interaction with the European
60 plate during the early stages of Adriatic trench retreat and backarc extension.

61 **GEOLOGIC BACKGROUND**

62 The Western Mediterranean orogenic belts record the progressive Meso-Cenozoic
63 convergence between Adria and Europe, and the consequent closure of the Tethyan
64 Ocean in between (Dewey et al., 1989; Jolivet et al., 2003; Handy et al., 2010; Malusà et
65 al., 2015). In the Alps-Apennines region, most of the Tethyan Ocean was subducted
66 beneath the Adriatic microplate in Cretaceous time (Zanchetta et al., 2015), until Alpine
67 subduction was choked by the arrival of thick European crust at the trench, followed by
68 late Eocene exhumation of (ultra)high pressure ((U)HP) rocks and by the emplacement of
69 Periadriatic magmatic rocks (Handy et al., 2010). (U)HP exhumation was likely triggered
70 by the northward motion of Adria relative to Europe (Malusà et al., 2015), which is still
71 documented during the Neogene when the Adriatic slab started retreating eastwards
72 (Faccenna et al., 2001), leading to the scissor-type opening of the Ligurian-Provençal
73 basin and to the counterclockwise rotation of Corsica-Sardinia, with a rotation pole
74 located in the northern Ligurian Sea (Wortel and Spakman, 2000; Gattacceca et al.,
75 2007). Meanwhile, the progressive indentation of Adriatic lithosphere beneath the Central

76 Alps led to the erosional unroofing of the Lepontine Dome (Garzanti and Malusà, 2008).
77 The Lepontine Dome includes two distinct subdomes of Cenozoic amphibolite-facies
78 metamorphic rocks (Ticino and Toce subdomes) that formed stepwise from east to west,
79 at a distance of ~50 km from each other, as a response to progressive Adria indentation
80 (Merle et al., 1989). The relative displacement between the Adriatic indenter and the
81 overlying Cenozoic metamorphic rocks was accommodated by the right-lateral Insubric
82 Fault (Merle et al., 1989; Schmid et al., 1989), while the focused erosion of the Ticino
83 and Toce subdomes provided huge amounts of detritus to the Adriatic foredeep turbidites,
84 which are now accreted in the Northern Apennines (~80% of total foredeep detritus,
85 according to petrographic and fission track data; Garzanti and Malusà, 2008). Therefore,
86 provenance changes in the Adriatic foredeep turbidites can be used to track the motion of
87 the Adriatic indenter beneath the Central Alps, and to constrain the age of major strike-
88 slip motion along the poorly dated Insubric Fault.

89 **METHODS**

90 Detrital zircon U-Pb geochronology provides an excellent means of detecting
91 provenance changes in the Adriatic foredeep turbidites, because of the markedly different
92 age signatures characterizing the Ticino and Toce subdomes in the Central Alps (Malusà
93 et al., 2013) (see kernel density estimates (KDE – Vermeesch, 2012) in Fig. 1). Detritus
94 shed from the Toce subdome (r1) is dominated by Variscan zircon U-Pb ages, whereas
95 detritus shed from the Ticino subdome (r2) is dominated by Caledonian zircon U-Pb ages
96 (Fig. 1). The overlying Cretaceous wedge (Zanchetta et al., 2015) additionally shows
97 abundant Precambrian ages and an age peak at 32–30 Ma (r3 in Fig. 1), corresponding to
98 the climax of Periadriatic magmatism. Resistance of zircon to diagenetic dissolution, and

99 the high closure temperature of the U-Pb geochronologic system, ensure that detrital
100 zircon signatures remain unchanged after burial and diagenesis.

101 Within this framework, we collected 11 sandstone samples for detrital zircon U-
102 Pb analysis from the proximal and distal successions of the Adriatic foredeep, exposed in
103 the Southern Alps and Northern Apennines, respectively (s1 to s11 in Fig. 1). The
104 stratigraphic ages of these samples are independently constrained by biostratigraphic data
105 (Catanzariti et al., 2002; Tremolada et al., 2010), ranging from 32 to 18 Ma, thus
106 covering the whole time interval relevant for the analyzed geodynamic processes. Distal
107 samples include those from the Aveto, Macigno, Modino and Bobbio formations.
108 Proximal samples include those from the Villa Olmo and Como formations of the
109 Gonfolite Group, fed by local sources encompassing the Bergell volcano-plutonic
110 complex and the Cretaceous-wedge country rocks (Malusà et al., 2011).

111 After conventional heavy mineral separation, all grains were mounted
112 (unpolished) on double-sided tape and depth profiled using laser ablation with a Photon
113 Machine Analyte G2 ArF 193 nm Excimer Laser in a large volume Helex cell. The
114 progressively ablated aerosol and He carrier gas were injected and analyzed using an
115 Element2 magnetic-sector ICP-MS. LA-ICPMS depth profiling allows for multiple ages
116 to be obtained from a single analysis, due to ablation of the grain normal to growth
117 zonation. A more detailed description of the analytical procedures is provided in the Data
118 Repository.

119 **RESULTS AND INTERPRETATIONS**

120 Results are summarized in Figure 2 (see Data Repository for raw U-Pb data).
121 Only rim ages are included in this figure, to allow for an unbiased comparison with the

122 data set published in Malusà et al. (2013), whereas both rim and core ages are included in
123 the Data Repository. Kernel density estimates (KDE in Fig. 2) show that the analyzed
124 samples include, in variable proportions, grain ages belonging to the Periadriatic,
125 Variscan, Caledonian and Precambrian populations, as observed in modern sands shed
126 from the potential source areas (Malusà et al., 2013).

127 Periadriatic zircon grains define a stationary peak (Malusà et al., 2011) observed
128 in all but one sample (s3). The range of Periadriatic ages is fully consistent with
129 published zircon U-Pb ages in Periadriatic magmatic rocks (Rosenberg, 2004). The age of
130 the youngest Periadriatic grains in each sample decreases upsection, and is systematically
131 older, as expected, than the stratigraphic age of the enclosing sedimentary rock.

132 The relative abundance of Periadriatic zircon grains exceeds 50% in samples
133 coeval with the climax of Periadriatic magmatism (Aveto Fm, s1 and s2), which are
134 dominated by volcanic zircon grains, and drops to 0% in samples deposited shortly after
135 the cessation of magmatic activity (s3). Then, the abundance of Periadriatic zircon grains
136 progressively increases upsection because of the progressive unroofing of the Bergell
137 volcano-plutonic complex (Figs. 1, 2) (Malusà et al., 2011). The abundance of
138 Periadriatic zircon grains largely exceeds 50% in proximal Aquitanian samples (s7 and
139 s8), reaches 45%–50% in coeval distal samples also fed by Lepontine sources (s9 and
140 s10), and decreases to 16% in the Burdigalian sample (s11).

141 Among the non-Periadriatic zircon grains, the relative abundance of Precambrian
142 grains is a good marker to discriminate more local sources feeding the proximal Adriatic
143 foredeep (47%–65% Precambrian grains in samples s5-s8) from the broader sources
144 feeding the distal Adriatic foredeep (14%–29% Precambrian grains in samples s1-s4 and

145 s9-s11). The former sources are in fact dominated by Cretaceous-wedge country rocks
146 presently drained by the River Adda, and particularly rich in Precambrian zircon grains,
147 whereas the latter also include the metamorphic subdomes presently drained by Rivers
148 Ticino and Toce, and containing a higher proportion of Phanerozoic (i.e., Variscan and
149 Caledonian) zircon grains.

150 Variations in Variscan versus Caledonian zircon grain abundance reveal major
151 provenance shifts within the Lepontine Dome during the analyzed time interval. The
152 Variscan/Caledonian zircon grain ratio is rather constant in distal samples during the
153 Oligocene (1.1–1.3), but sharply increases (up to >5) at ~24–23 Ma (Fig. 2). This
154 indicates that detritus supplied from the Toce subdome became overwhelming at that
155 time, i.e., since the Aquitanian. When considering that zircon fertility in bedrock is much
156 lower in the Toce drainage (12 ppm) than in the Ticino and Adda drainages (68 and 36
157 ppm, respectively), this change in provenance is even more relevant because sediment
158 contribution from the Toce subdome is prone to be underestimated in the detrital
159 geochronology record (Malusà et al., 2016a). Insofar as westward motion of the Adriatic
160 indenter was accommodated by strike-slip along the Insubric Fault, and also caused the
161 uplift and exhumation of the Toce dome, we infer that both of these tectonic events must
162 have occurred at ~24–23 Ma.

163 An alternative explanation for this sharp provenance change may invoke a
164 broader paleodrainage reorganization. At ~24–23 Ma, the drainage system was already
165 established in the Lepontine Dome (Garzanti and Malusà, 2008), but not in the Paleogene
166 and Cretaceous wedges. However, a major impact of the Paleogene wedge into the zircon
167 geochronology record of the Adriatic foredeep can be excluded for the following reasons:

168 (i) the zircon fertility in the Paleogene wedge is much lower than in the Lepontine Dome
169 (Malusà et al., 2016a); (ii) the Paleogene wedge lacks of Periadriatic magmatic rocks, and
170 cannot provide the Periadriatic signal observed in the Adriatic foredeep; (iii) large areas
171 of the Paleogene wedge were not eroded, but covered by wedge-top sediments at ~24–23
172 Ma (Malusà and Balestrieri, 2012). Most of the Cretaceous wedge also underwent
173 negligible erosion during the Neogene, as attested by the widespread preservation of
174 volcanic and subvolcanic rocks (Zanchetta et al., 2015).

175 **DISCUSSION**

176 Detrital zircon U-Pb age data on foredeep turbidites indicate that the westward
177 shift of the Adriatic indenter beneath the Central Alps took place at 24–23 Ma. Therefore,
178 it is broadly coeval with the onset of Apenninic trench retreat and backarc extension on
179 top of the subducting Adriatic slab (e.g, Faccenna et al., 2001; Gattacceca et al., 2007).
180 At the same time, Adria (and Africa) was moving northward relative to Europe, as
181 documented by plate motion constraints (Dewey et al., 1989, purple arrows in Fig. 3A).
182 Coexistence of right-lateral slip on the northern boundary of the Adriatic microplate, and
183 of trench retreat during scissor-type opening of the backarc basin to the west, requires a
184 near-vertical rotation axis located at the northern tip of the Ligurian-Provençal basin, in
185 agreement with paleomagnetic data (Gattacceca et al., 2007). On the basis of the new
186 time constraints for the strike-slip motion along the Insubric Fault, we propose that the
187 position of such a rotation axis was controlled by the interaction at depth between the
188 European slab to the north, and the Adriatic slab to the south. These two slabs possibly
189 collided at depth by the end of the Oligocene, hindering the northward propagation of the
190 Adriatic indenter and triggering its westward shift beneath the Central Alps (Fig. 3A).

191 The proposed geodynamic scenario can be tested by using available plate-motion
192 constraints and recent palinspastic reconstructions (Malusà et al., 2015; 2016b). Low-
193 temperature thermochronology data from Corsica-Sardinia (Malusà et al., 2016b) attest
194 that the northern tip of the Adriatic slab was located offshore northern Corsica at ~23 Ma.
195 Therefore, during Alpine subduction, ~300 km distance separated the Central Alps trench
196 from the northern tip of the Adriatic slab to the south. This requires at least >400 km
197 convergence at the Central Alps trench in order to account for both the vertical and
198 horizontal components of subduction, before having a possible interaction between the
199 south-dipping European slab and the west-dipping Adriatic slab. The diagram in Figure
200 3B shows that the amount of convergence estimated at the Central Alps trench during the
201 last 80 Ma is fully consistent with this requirement.

202 The interaction between the European and Adriatic slabs proposed in this work
203 explains not only the sudden westward shift of the Adriatic indenter, but also: (i) the
204 location of the Corsica-Sardinia rotation pole inferred by paleomagnetic data; (ii) the
205 location of the northern tip of the fan-shaped Ligurian-Provençal basin; and (iii) the
206 foreland-ward propagation of Alpine deformation in the Neogene, when convergence was
207 no longer accommodated along the Alpine trench because of slab interaction at depth.

208 **SUMMARY AND CONCLUSIONS**

209 Detrital zircon U-Pb geochronology on Adriatic foredeep turbidites constrains
210 both the age of the westward shift of the Adriatic indenter beneath the Central Alps, and
211 the associated strike-slip motion along the Insubric Fault, to ~24–23 Ma. Therefore,
212 right-lateral slip on the northern boundary of the Adriatic microplate was coeval with
213 trench retreat in the Apennines and with scissor-type backarc opening in the Ligurian-

214 Provençal basin. This requires a near-vertical rotation axis at the northern tip of the
215 Ligurian-Provençal basin, consistent with paleomagnetic data, and possibly controlled by
216 the interaction at depth between the European and the Adriatic slabs. Our results provide
217 new pin-points to the recent geodynamic reconstructions of the Western Mediterranean,
218 and confirm that detrital zircon U-Pb geochronology can be successfully employed to
219 investigate the linkage between surface and deep-seated tectonic processes in complex
220 geodynamic settings.

221 **ACKNOWLEDGMENTS**

222 We thank J.A. Spotila, P.G. DeCelles, A. Leier, and an anonymous reviewer for
223 their insightful comments, G. Ottria for assistance during sampling, L. Stockli and S.
224 Seaman for help with laboratory procedures, and the Jackson School of Geoscience
225 (University of Texas at Austin) for providing financial support to the project.

226 **REFERENCES CITED**

- 227 Catanzariti, R., Ottria, G., and Cerrina Feroni, A., 2002, Carta Geologico-Strutturale
228 dell'Appennino Emiliano-Romagnolo. Tavole Stratigrafiche: SELCA, Firenze, 92 p.
- 229 Dewey, J.F., Helman, M.L., Turco, E., Hutton, D.H.W., and Knott, S.D., 1989,
230 Kinematics of the western Mediterranean, *in* Coward, M.P., Dietrich, D., and Park,
231 R.G., eds., Alpine tectonics: Geological Society, London, Special Publication 45, p.
232 265–283.
- 233 Faccenna, C., Becker, T.W., Lucente, F.P., Jolivet, L., and Rossetti, F., 2001, History of
234 subduction and back arc extension in the Central Mediterranean: Geophysical
235 Journal International, v. 145, p. 809–820, doi:10.1046/j.0956-540x.2001.01435.x.

- 236 Garzanti, E., and Malusà, M.G., 2008, The Oligocene Alps: Domal unroofing and
237 drainage development during early orogenic growth: *Earth and Planetary Science*
238 *Letters*, v. 268, p. 487–500, doi:10.1016/j.epsl.2008.01.039.
- 239 Gattacceca, J., Deino, A., Rizzo, R., Jones, D.S., Henry, B., Beaudoin, B., and Vadeboin,
240 F., 2007, Miocene rotation of Sardinia: New paleomagnetic and geochronological
241 constraints and geodynamic implications: *Earth and Planetary Science Letters*,
242 v. 258, p. 359–377, doi:10.1016/j.epsl.2007.02.003.
- 243 Handy, M.R., Schmid, S.M., Bousquet, R., Kissling, E., and Bernoulli, D., 2010,
244 Reconciling plate-tectonic reconstructions of Alpine Tethys with the geological-
245 geophysical record of spreading and subduction in the Alps: *Earth-Science Reviews*,
246 v. 102, p. 121–158, doi:10.1016/j.earscirev.2010.06.002.
- 247 Jolivet, L., Faccenna, C., Goffé, B., Burov, E., and Agard, P., 2003, Subduction tectonics
248 and exhumation of high-pressure metamorphic rocks in the Mediterranean orogens:
249 *American Journal of Science*, v. 303, p. 353–409, doi:10.2475/ajs.303.5.353.
- 250 Malusà, M.G., and Balestrieri, M.L., 2012, Burial and exhumation across the Alps–
251 Apennines junction zone constrained by fission-track analysis on modern river
252 sands: *Terra Nova*, v. 24, p. 221–226, doi: 10.1111/j.1365-3121.2011.01057.x
- 253 Malusà, M.G., Villa, I.M., Vezzoli, G., and Garzanti, E., 2011, Detrital geochronology of
254 unroofing magmatic complexes and the slow erosion of Oligocene volcanoes in the
255 Alps: *Earth and Planetary Science Letters*, v. 301, p. 324–336,
256 doi:10.1016/j.epsl.2010.11.019.

- 257 Malusà, M.G., Carter, A., Limoncelli, M., Villa, I.M., and Garzanti, E., 2013, Bias in
258 detrital zircon geochronology and thermochronometry: *Chemical Geology*, v. 359,
259 p. 90–107, doi:10.1016/j.chemgeo.2013.09.016.
- 260 Malusà, M.G., Faccenna, C., Baldwin, S.L., Fitzgerald, P.G., Rossetti, F., Balestrieri,
261 M.L., Danišík, M., Ellero, A., Ottria, G., and Piromallo, C., 2015, Contrasting styles
262 of (U)HP rock exhumation along the Cenozoic Adria-Europe plate boundary
263 (Western Alps, Calabria, Corsica): *Geochemistry Geophysics Geosystems*, v. 16,
264 p. 1786–1824, doi:10.1002/2015GC005767.
- 265 Malusà, M.G., Resentini, A., and Garzanti, E., 2016a, Hydraulic sorting and mineral
266 fertility bias in detrital geochronology: *Gondwana Research*, (in press),
267 doi:10.1016/j.gr.2015.09.002.
- 268 Malusà, M.G., Danišík, M., and Kuhleemann, J., 2016b, Tracking the Adriatic-slab travel
269 beneath the Tethyan margin of Corsica-Sardinia by low-temperature
270 thermochronometry: *Gondwana Research*, (in press), doi:10.1016/j.gr.2014.12.011.
- 271 Merle, O., Cobbold, P.R., and Schmid, S., 1989, Tertiary kinematics in the Lepontine
272 dome, *in* Coward, M.P., Dietrich, D., and Park, R.G., eds., *Alpine tectonics:*
273 *Geological Society, London, Special Publication 45*, p. 113–134.
- 274 Rosenberg, C.L., 2004, Shear zones and magma ascent: A model based on a review of the
275 Tertiary magmatism in the Alps: *Tectonics*, v. 23, TC3002,
276 doi:10.1029/2003TC001526.
- 277 Schmid, S.M., Aebli, H.R., Heller, F., and Zingg, A., 1989, The role of the Periadriatic
278 Line in the tectonic evolution of the Alps, *in* Coward, M.P., Dietrich, D., and Park,

- 279 R.G., eds., Alpine tectonics: Geological Society, London, Special Publication 45, p.
280 153–171, doi:10.1144/GSL.SP.1989.045.01.08.
- 281 Steck, A., and Hunziker, J., 1994, The Tertiary structural and thermal evolution of the
282 Central Alps – compressional and extensional structures in an orogenic belt:
283 Tectonophysics, v. 238, p. 229–254, doi:10.1016/0040-1951(94)90058-2.
- 284 Tremolada, F., Guasti, E., Scardia, G., Carcano, C., Rogledi, S., and Sciunnach, D., 2010,
285 Reassessing the biostratigraphy and the paleobathymetry of the Gonfolite Lombarda
286 Group in the Como area (northern Italy): Rivista Italiana di Paleontologia e
287 Stratigrafia, v. 116, p. 35–49.
- 288 Vermeesch, P., 2012, On the visualisation of detrital age distributions: Chemical
289 Geology, v. 312-313, p. 190–194, doi:10-1016/j.chemgeo.2012.04.021.
- 290 Wortel, M.J.R., and Spakman, W., 2000, Subduction and slab detachment in the
291 Mediterranean-Carpathian region: Science, v. 290, p. 1910–1917,
292 doi:10.1126/science.290.5498.1910.
- 293 Zanchetta, S., Malusà, M.G., and Zanchi, A., 2015, Precollisional development and
294 Cenozoic evolution of the Southalpine retrobelt (European Alps): Lithosphere, v. 7,
295 p. 662–681, doi:10.1130/L466.1.
- 296 Zwingmann, H., and Mancktelow, N., 2004, Timing of Alpine fault gouges: Earth and
297 Planetary Science Letters, v. 223, p. 415–425, doi:10.1016/j.epsl.2004.04.041.

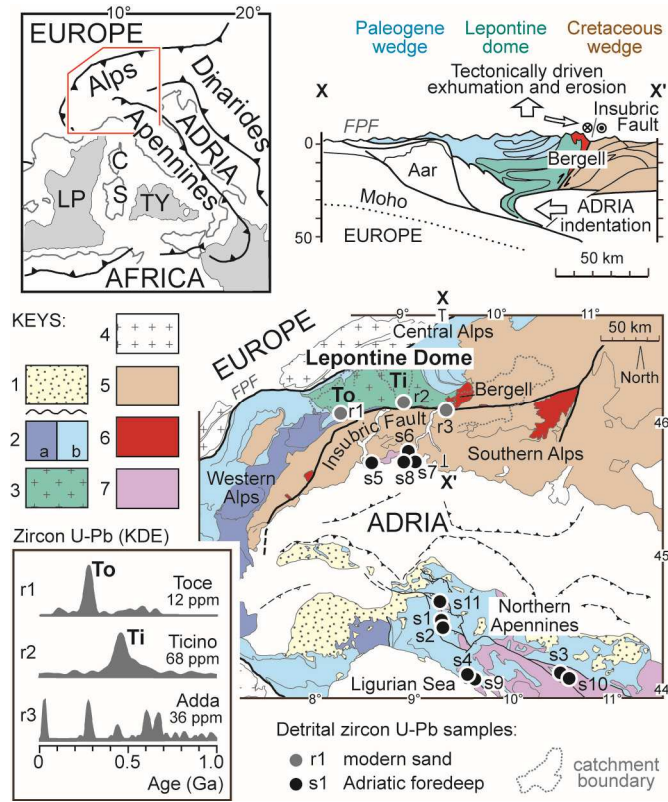
298

299 FIGURE CAPTIONS

300

301

302

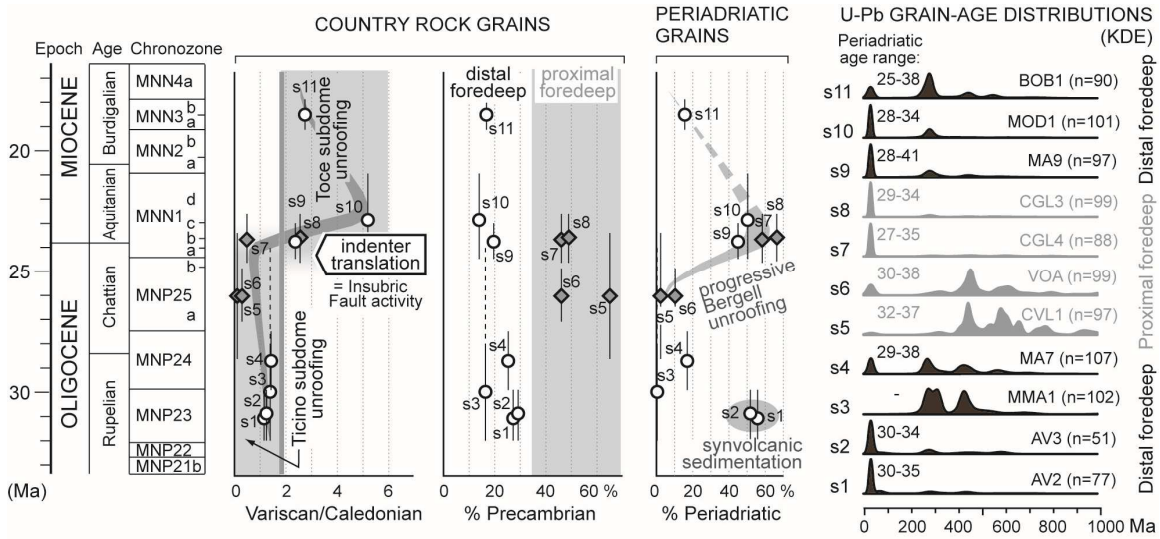


303

304 Figure 1. Geologic map of the study area with sample locations, cross section across the
 305 Central Alps (top-right), and tectonic sketch map of the Western Mediterranean (top-left)
 306 (modified from Malusà et al., 2015). Keys: 1, wedge-top successions; 2, Paleogene
 307 wedge (a, (U)HP belt; b, lower-grade units); 3, Lepontine Dome; 4, External Massifs; 5,
 308 Cretaceous wedge (Austroalpine and Southalpine sequences); 6, Periadriatic intrusives; 7,
 309 Adriatic foredeep turbidites, Subligurian and Tuscan units. Acronyms: C, Corsica; FPF,
 310 Frontal Pennine Fault; LP, Ligurian-Provençal basin; S, Sardinia; Ti, Ticino subdome;
 311 To, Toce subdome; TY, Tyrrhenian basin. Zircon U-Pb kernel density estimates on
 312 modern sands (KDE, bottom-left) are from Malusà et al. (2013), zircon fertility values
 313 (ppm) in each drainage are from Malusà et al. (2016a).

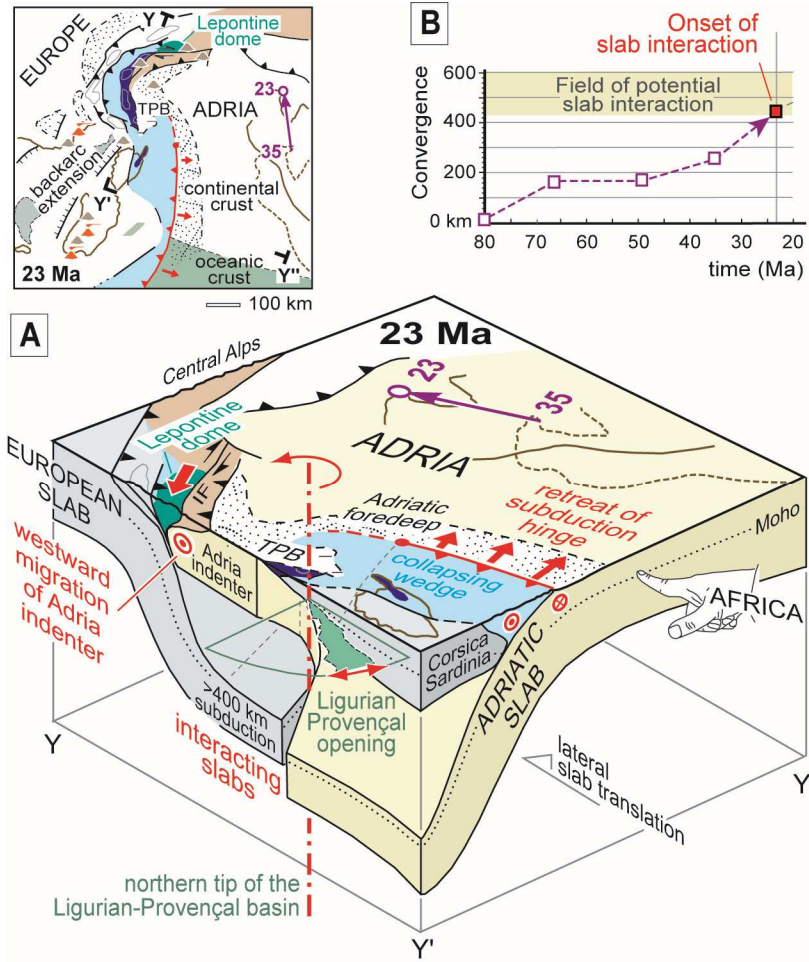
314

315



316

317 Figure 2. Ratio of Variscan versus Caledonian zircon grains, and percentage of
 318 Precambrian and Periadriatic grains in samples s1 to s11 (chronozones after Catanzariti et
 319 al., 2002). Note the sharp provenance change during the Oligocene-Miocene transition.
 320 On the right, kernel density estimates (KDE) including the age range of the Periadriatic
 321 populations (in Ma), and the number of analyzed grains in each sample (n) (only
 322 concordant ages < 1Ga are shown in the KDEs).



323

324 Figure 3. A) 3D configuration of the interacting European and Adriatic slabs during the
325 westward migration of the Adriatic indenter, the onset of slab retreat, and the scissor-type
326 opening of the Ligurian-Provençal basin (no vertical exaggeration; see location in the
327 palinspastic map on the top left, from Malusà et al., 2015). IF, Insubric Fault; TPB,
328 Tertiary Piedmont Basin; purple arrows = trajectories of Adria motion relative to Europe
329 (numbers = age in Ma). B) Convergence history at the Central Alps trench (based on
330 Malusà et al., 2015) as compared with the amount of convergence required for slab
331 interaction.

332

333 ¹GSA Data Repository item 2016xxx, sample locations, detailed analytical methods, and
334 raw U-Pb data, is available online at www.geosociety.org/pubs/ft2015.htm, or on request
335 from editing@geosociety.org or Documents Secretary, GSA, P.O. Box 9140, Boulder,
336 CO 80301, USA.